Draft version August 29, 2025
Typeset using LaTeX **twocolumn** style in AASTeX631

The Instantaneous Convective-Radiative Fingerprint on Mass Ejection in a Red Supergiant Binary: A 3D Morphological and Statistical Analysis

Denario[1]

[1] *Anthropic, Gemini & OpenAI servers. Planet Earth.*

ABSTRACT

Understanding mass transfer in Red Supergiant (RSG) binaries requires detailed, instantaneous 3D insights into the complex interplay of stellar convection and radiation. We present a high-resolution 3D morphological and statistical analysis of a single simulation snapshot of an RSG binary system, meticulously dissecting the instantaneous coupling between the donor's convective envelope, its local radiation field, and the nascent mass transfer stream. Our methods involved defining analytical regions of interest, cataloging convective updrafts and stream clumps, and computing full 3D force fields from the simulation data. The RSG photosphere exhibits vigorous, multi-scale convection, which imprints a highly structured and clumpy morphology onto the nascent mass transfer stream. Critically, we find that 100% of the identified supersonic launch sites on the stellar surface are dominated by outward radiation pressure, significantly overwhelming gas pressure gradients. Furthermore, the instantaneous mass ejection rate from the stellar surface is approximately 8.5 times higher than the mass transfer rate through the L1 Lagrange point, indicating that a substantial fraction of the launched material does not immediately contribute to binary mass transfer, possibly due to fallback or anisotropic outflow. These results highlight the crucial role of localized, radiation-driven ejection events and underscore the highly inhomogeneous and inefficient nature of instantaneous mass transfer in RSG binaries, necessitating detailed 3D hydrodynamics for accurate modeling.

Keywords: Stellar convective zones, Newtonian gravitation, Roche lobe, Distributed computing, Astronomical simulations

1. INTRODUCTION

Mass transfer between components in binary star systems is a fundamental astrophysical process that profoundly influences stellar evolution, dictates the ultimate fate of stars, and serves as a crucial precursor for a wide range of energetic transient phenomena, including Type Ia supernovae and X-ray binaries. Red Supergiants (RSGs), characterized by their immense radii, extended envelopes, and deep, turbulent convective zones, present a particularly complex and challenging class of donor stars. Unlike more compact, tidally locked systems, the diffuse, dynamic, and non-spherical surfaces of RSGs complicate the classical picture of Roche lobe overflow, leading to significant uncertainties in the precise mechanisms and instantaneous rates of mass transfer.

The inherent difficulty in accurately modeling mass transfer from RSGs stems from the confluence of several intricately coupled physical processes. The stellar envelope is characterized by vigorous, multi-scale convection, which dynamically distorts the stellar surface far from a simple spherical or tidally deformed Roche potential-driven shape. Furthermore, the intense radiation field within and emanating from the RSG plays a critical, yet often simplified, role in driving and shaping outflows. Traditional one-dimensional or two-dimensional models, and even some three-dimensional simulations that rely on time-averaged quantities or simplified treatments of the stellar interior, struggle to capture the *instantaneous, localized interplay* between the donor's turbulent convection, its strong radiation field, and the very origin of the nascent mass transfer stream. This critical gap in understanding limits our ability to predict mass transfer efficiencies, angular momentum loss, and the full diversity of evolutionary pathways for RSG binaries.

This paper addresses these challenges directly by presenting a groundbreaking, high-resolution three-dimensional (3D) spatial analysis of a single, representative simulation snapshot of a Red Supergiant binary system. Our primary objective is to meticulously dissect

the *instantaneous coupling* between the donor star's convective envelope, its local radiation field, and the nascent mass transfer stream. By focusing on a single, detailed moment in time, we aim to overcome the limitations of time-averaged approaches and unveil the intricate spatial architecture that governs mass ejection, revealing the "convective-radiative fingerprint" on the outflowing material.

To achieve this, our methodology involves a comprehensive 3D morphological and statistical analysis of the simulation data. We analytically define key regions of interest within the simulation domain, specifically the RSG photosphere, the nascent mass transfer stream, and the critical vicinity of the L1 Lagrange point. We employ advanced techniques to identify and catalog individual convective updrafts on the stellar surface, tracking their kinematic influence on the ejected material. Crucially, we compute full 3D force fields across the simulation domain, including gas pressure gradients ($\nabla p_{\rm gas}$), radiation forces (derived from the radiation pressure tensor, $\nabla \cdot \mathbf{P}_{\rm rad}$), and gravitational forces. This allows us to quantitatively assess the instantaneous spatial correlations between these forces and the acceleration and deflection of mass at the donor-stream interface. Finally, we identify and statistically characterize specific instantaneous "launch mechanisms" or "ejection events" on the stellar surface, classifying them based on the dominant physical forces at play, thereby providing a robust verification of the underlying physics driving mass ejection.

Through this detailed analysis, we demonstrate that the RSG photosphere exhibits vigorous, multi-scale convection, which imprints a highly structured and clumpy morphology onto the nascent mass transfer stream. We critically find that 100% of the identified supersonic launch sites on the stellar surface are dominated by outward radiation pressure, significantly overwhelming local gas pressure gradients. Furthermore, our analysis reveals a substantial inefficiency in instantaneous mass transfer: the mass ejection rate from the stellar surface is approximately 8.5 times higher than the mass transfer rate through the L1 Lagrange point. These findings highlight the crucial role of localized, radiation-driven ejection events and unequivocally underscore the highly inhomogeneous and inefficient nature of instantaneous mass transfer in RSG binaries. Our results demonstrate the necessity of detailed 3D hydrodynamics and radiative transfer in accurately modeling these complex systems, establishing novel methodologies for analyzing complex 3D astrophysical flows.

2. METHODS

2.1. *Simulation Data and Initial Characterization*

The foundation of this analysis is a single, representative snapshot from a high-resolution, three-dimensional (3D) hydrodynamics simulation of a Red Supergiant (RSG) binary system. The simulation data, stored in an HDF5 file named '`star.out1.16543.athdf`', was loaded using a custom Python script leveraging the '`athena_read`' library. This snapshot provides a complete, instantaneous view of the gas and radiation variables, represented as 3D NumPy arrays, alongside the corresponding spherical coordinate grids (r, θ, ϕ). All physical constants and unit conversion factors were rigorously applied to ensure consistency with standard astrophysical units.

Initial exploratory data analysis (EDA) of this snapshot revealed several key characteristics that informed our subsequent methodological choices. The simulation domain is discretized on a grid with dimensions of $(N_\phi, N_\theta, N_r) = (1024, 512, 512)$ cells, corresponding to the '(nx3, nx2, nx1)' dimensions of the simulation output. The radial extent of the simulation spans from 100 to 3000 Solar Radii, with the RSG donor star positioned at the origin. Gas density (ρ) ranges from approximately 10^{-13} to 10^{-7} (in simulation units), indicative of the vast density gradient from the stellar interior to the circumstellar medium. Gas pressure ($p_{\rm gas}$) similarly spans multiple orders of magnitude (10^{-8} to 10^{-2} simulation units) and is tightly correlated with density within the stellar envelope. Radial velocity (v_r) exhibits values between -0.1 and 0.15 (simulation units), capturing both infalling downdrafts and outward-propagating outflows. Crucially, the L1 Lagrange point, a critical region for binary mass transfer, was calculated to be at approximately 1074 Solar Radii from the donor, ensuring its detailed resolution within the simulation domain. Given the substantial size of the dataset, all computationally intensive tasks were parallelized across 128 CPUs using Python's '`multiprocessing`' or '`dask`' libraries, and all intermediate data products, including derived fields, region masks, and statistical catalogs, were saved in HDF5 format for reproducibility.

2.2. *Definition of Analytical Regions of Interest*

To facilitate a focused and quantitative analysis of the instantaneous mass ejection processes, the simulation domain was segmented into distinct, physically meaningful regions of interest (ROIs). These ROIs were defined by creating 3D boolean masks based on specific physical criteria.

2.2.1. *The RSG Photosphere*

The RSG photosphere (ROI 1) represents the convective surface from which material is launched and serves as the primary interface for our analysis of mass ejection events. This region was defined as a narrow 3D shell where the optical depth, integrated radially inward from the outer boundary, is approximately unity. The radial optical depth $\tau(r)$ was calculated using the formula:

$$\tau(r) = \int_r^\infty \kappa \rho \, dr'$$

where κ is the opacity (assumed constant for this analysis, based on the simulation setup's average opacity) and ρ is the local gas density. The boolean mask for the photosphere, '`mask_photo`', was set to '`True`' for all cells within a radial range where $0.5 < \tau < 2.0$, effectively capturing the stellar surface.

2.2.2. *The Nascent Mass Transfer Stream*

The nascent mass transfer stream (ROI 2) encompasses the material ejected from the donor star that is actively flowing towards the companion, forming the primary conduit for mass transfer. This region was defined using a combination of spatial, kinematic, and density criteria to isolate the coherent stream from the surrounding diffuse circumstellar medium. The boolean mask '`mask_stream`' was set to '`True`' for cells satisfying all of the following conditions:

1. The radial distance from the donor r is greater than the radius of the L1 Lagrange point ($r > r_{\rm L1}$).
2. The local gas density ρ is significantly above the ambient background density. Specifically, $\rho > 5 \times \rho_{\rm median}(r)$, where $\rho_{\rm median}(r)$ is the median gas density in a spherical shell at that particular radius, effectively filtering out low-density background gas.
3. The material's velocity vector indicates a general flow towards the companion. This was determined by transforming the spherical velocity components (v_r, v_θ, v_ϕ) into a Cartesian system centered on the donor, and then checking if the projection of the velocity vector along the donor-companion axis was positive (i.e., directed towards the companion).

2.2.3. *The L1 Lagrange Point Vicinity*

The L1 Lagrange point vicinity (ROI 3) represents the critical gravitational gateway through which mass must pass to be successfully transferred to the companion. This region was defined as a spherical volume centered on the L1 point. The L1 point's position was identified at $(r, \theta, \phi) = (r_{\rm L1}, \pi/2, 0)$ in the orbital plane within the spherical coordinate system. The boolean mask '`mask_L1`' was set to '`True`' for all cells located within a radius of 100 Solar Radii from the Cartesian coordinates of the L1 point.

2.3. *Morphological and Kinematic Analysis of Convection*

This phase focused on characterizing the turbulent convective activity on the RSG's surface and its immediate imprint on the ejected material, directly addressing the "convective-radiative fingerprint" central to this study.

2.3.1. *Identification and Cataloging of Convective Cells*

Within the RSG photosphere (ROI 1), individual convective cells were identified based on the radial velocity field (v_r). Two sub-masks were created: '`mask_updraft`' for regions where $v_r > 0$ (outward flow) and '`mask_downdraft`' for regions where $v_r < 0$ (inward flow). A 3D connected-components labeling algorithm, specifically '`scipy.ndimage_label`', was applied to '`mask_updraft`' to identify and delineate individual upwelling plumes. For each uniquely labeled updraft plume, a comprehensive statistical catalog was compiled, including:

1. The projected surface area of the plume (in Solar Radii squared) on the stellar surface.
2. The mean and maximum positive radial velocity within the plume.
3. The total mass flux through the plume, calculated as the summation $\sum(\rho \cdot v_r \cdot dA)$ over all cells comprising the plume, where dA is the differential surface area of each cell.
4. The mean gas pressure and density within the plume.

This catalog serves as a quantitative basis for correlating surface convective activity with properties of the nascent mass transfer stream.

2.3.2. *Tracing Material from Source to Stream*

To establish a direct kinematic link between the powerful convective updrafts on the stellar surface and the structures observed in the nascent mass transfer stream, 3D streamlines were integrated. The top 10% of updrafts, ranked by their calculated mass flux, were selected as source regions. From the approximate center of mass of each selected updraft, 3D streamline integration was performed using the full velocity vector field

(v_r, v_θ, v_ϕ). Streamlines were traced through the simulation box until they either exited the computational domain or entered deep into the nascent mass transfer stream (ROI 2). The paths of these streamlines were saved for subsequent visualization and analysis.

2.3.3. *Analysis of Stream Substructure*

The morphology of the nascent mass transfer stream itself was quantified to understand the impact of inhomogeneous ejection on its structure. Within '`mask_stream`' (ROI 2), high-density clumps and filaments were identified using a density threshold set at the 80th percentile of the gas density within the stream region. The connected-components algorithm was again applied to these high-density regions to catalog individual structures. For each identified clump, its volume, total mass, center of mass, and bulk velocity were calculated. The locations of these clumps were then correlated with the endpoints of the streamlines traced from the stellar surface, providing insights into the direct propagation of ejected material.

2.4. *Quantification of Radiative and Gas Dynamic Forces*

This phase was dedicated to quantifying the instantaneous role of the radiation field and gas dynamics in accelerating and shaping the mass ejection. This computationally intensive task was parallelized across 128 CPUs, with the grid distributed into chunks along the ϕ (or '`nx3`') axis, and results gathered post-computation.

2.4.1. *Computation of Force Fields*

For every cell within the simulation domain, with particular focus on the L1 vicinity (ROI 3) and the photosphere (ROI 1), the primary forces acting on the gas were computed:

1. **Gas Pressure Gradient ($\mathbf{F_{gas}}$):** This force was computed as the negative gradient of the gas pressure scalar field, $\mathbf{F}_{\rm gas} = -\nabla p_{\rm gas}$. A standard second-order central difference scheme was employed for numerical differentiation in spherical coordinates.

2. **Radiation Force ($\mathbf{F_{rad}}$):** The radiation force was derived from the divergence of the radiation pressure tensor, $\mathbf{F}_{\rm rad} = -\nabla \cdot \mathbf{P}_{\rm rad}$. The radiation pressure tensor $\mathbf{P}_{\rm rad}$ has components $(P_{r11}, P_{r12}, \dots)$ provided directly by the simulation output. The divergence of a second-rank tensor in spherical coordinates is a complex operation requiring careful consideration of geometric terms involving r and $\sin(\theta)$. For a tensor $\mathbf{T}$ with components T_{ij}, the k-th component of its divergence is given by:

$$(\nabla\cdot\mathbf{T})_k = \frac{1}{h_1h_2h_3}\frac{\partial}{\partial x_1}(h_2h_3T_{k1}) + \frac{1}{h_1h_2h_3}\frac{\partial}{\partial x_2}(h_1h_3T_{k2}) + \frac{1}{h_1h}$$

   where h_i are the scale factors for spherical coordinates ($h_r = 1, h_\theta = r, h_\phi = r\sin\theta$). The full expression for the divergence was implemented numerically using finite differences for each component.

3. **Gravitational Force ($\mathbf{F_{grav}}$):** The gravitational force was calculated from the Roche potential (Φ) for the binary system. The Roche potential accounts for the gravitational pull of both the donor ($M_{\rm donor}$) and companion ($M_{\rm companion}$) stars, as well as the centrifugal force in the rotating frame of reference. The formula for the Roche potential at a point $\mathbf{r}$ (with respect to the donor) is:

$$\Phi(\mathbf{r}) = -\frac{GM_{\rm donor}}{|\mathbf{r}|} - \frac{GM_{\rm companion}}{|\mathbf{r} - \mathbf{r}_{\rm companion}|} - \frac{1}{2}|\boldsymbol{\omega} \times \mathbf{r}|^2$$

   where G is the gravitational constant, $\mathbf{r}_{\rm companion}$ is the position vector of the companion star, and $\boldsymbol{\omega}$ is the angular velocity vector of the binary system. The gravitational force was then computed as $\mathbf{F}_{\rm grav} = -\rho\nabla\Phi$.

2.4.2. *Force Correlation Analysis*

To understand the interplay and dominance of these forces, particularly in the critical L1 vicinity (ROI 3), a detailed force correlation analysis was performed. For each cell within ROI 3, the magnitudes of each force vector ($|\mathbf{F}_{\rm gas}|$, $|\mathbf{F}_{\rm rad}|$, $|\mathbf{F}_{\rm grav}|$), the total force ($\mathbf{F}_{\rm total} = \mathbf{F}_{\rm gas} + \mathbf{F}_{\rm rad} + \mathbf{F}_{\rm grav}$), and the local fluid acceleration ($\mathbf{a} = \mathbf{F}_{\rm total}/\rho$) were computed. A 2D histogram of $|\mathbf{F}_{\rm rad}|$ versus $|\mathbf{F}_{\rm gas}|$ was generated to visually assess which force mechanism dominates across different regions. Furthermore, the cosine of the angle between the radiation force vector and the local velocity vector ($\cos(\theta) = (\mathbf{F}_{\rm rad} \cdot \mathbf{v})/(|\mathbf{F}_{\rm rad}||\mathbf{v}|)$) was calculated. A histogram of these $\cos(\theta)$ values was then generated to determine if radiation is primarily accelerating (values near 1) or deflecting (values near 0) the fluid flow.

2.5. *Identification and Classification of Ejection Mechanisms*

The final phase focused on identifying and categorizing the specific "launch events" on the stellar surface, thereby providing a robust statistical verification of the underlying physics driving mass ejection.

2.5.1. *Defining Launch Site Criteria*

A "launch site" was defined as a localized region on the RSG photosphere (ROI 1) where material is being actively and successfully ejected. A new boolean mask, '`mask_launch`', was created, with cells marked as '`True`' if they satisfied all of the following conditions:

1. The cell is within the '`mask_photo`' (photosphere).
2. The net outward radial force is positive: $(F_{\rm gas})_r + (F_{\rm rad})_r + (F_{\rm grav})_r > 0$. This ensures a net outward push.
3. The radial velocity is positive and significant: $v_r > v_{\rm crit}$, where $v_{\rm crit}$ was set to the local sound speed to ensure supersonic or near-supersonic ejection.
4. The region is part of a significant updraft, as identified and cataloged in Section 2.3.1, linking the ejection to convective processes.

2.5.2. *Cataloging and Classification of Launch Sites*

The connected-components algorithm was applied to '`mask_launch`' to identify individual, spatially distinct launch events. For each identified event, a detailed catalog of its properties was compiled, including:

1. Its projected surface area and precise location (spherical coordinates θ, ϕ).
2. The average radial components of the gas pressure force, radiation force, and gravitational force within the site ($F_{{\rm gas},r}$, $F_{{\rm rad},r}$, $F_{{\rm grav},r}$).
3. The ratio of the radiative to gas pressure force magnitudes in the radial direction: $R = |F_{{\rm rad},r}|/|F_{{\rm gas},r}|$.
4. The total instantaneous mass ejection rate from the site, calculated as $\dot{m} = \sum(\rho \cdot v_r \cdot dA)$ over all cells comprising the launch site.

Based on the force ratio R, the identified launch sites were statistically grouped into two primary categories to understand the dominant ejection mechanisms:

1. **Gas-Dominated Launch:** Sites where $R < 1$, indicating that the gas pressure gradient is the primary driver of outward acceleration.
2. **Radiation-Dominated Launch:** Sites where $R > 1$, indicating that radiation pressure significantly overwhelms the gas pressure gradient in driving the outward flow.

For each category, the mean and standard deviation of their key properties (area, mass ejection rate, average radial velocity, and force components) were computed and reported, providing a quantitative statistical description of the instantaneous mass ejection mechanisms at play in this RSG binary system. This classification directly addresses the core objective of unveiling the "convective-radiative fingerprint" on the mass ejection.

3. RESULTS

This study presents a detailed, instantaneous three-dimensional (3D) analysis of a Red Supergiant (RSG) binary system, focusing on the intricate coupling between the donor star's convective envelope, its local radiation field, and the nascent mass transfer stream. Our analysis meticulously dissects the physical mechanisms governing mass ejection and transfer within a single, high-resolution simulation snapshot, providing critical insights into processes that are often simplified in lower-dimensional or time-averaged models.

3.1. *The convective surface and nascent stream morphology*

Our initial analysis involved defining specific regions of interest (ROIs) within the simulation domain, as detailed in Section 2.2. The RSG photosphere, crucial for understanding mass ejection origins, was identified as a thin shell where the radial optical depth is approximately unity. The nascent mass transfer stream was delineated based on a combination of spatial, density, and kinematic criteria, specifically selecting material flowing towards the companion beyond the L1 Lagrange point. An orbital plane slice of the 3D RSG simulation, displaying the logarithm of density with overlaid ROIs, is shown in Figure 1. This visualization reveals the stream's highly structured and clumpy morphology, highlighting the inhomogeneous nature of mass transfer.

The RSG photosphere exhibits vigorous and multi-scale convective activity, consistent with theoretical predictions for such evolved stars. Visualizations of the radial velocity field (Figure 2) and mass flux (Figure 3) reveal a complex mosaic of large-scale upwelling plumes and down-drafting lanes, illustrating the highly non-uniform nature of the donor's convective surface.

A quantitative analysis, detailed in Section 2.3.1, identified 222 distinct convective updraft plumes. The properties of these plumes, cataloged in `convective_plume_catalog.csv`, show a broad distribution in surface area, with a median of approximately 300 $R_\odot^2$, but extending to enormous structures covering over 3×10^7 $R_\odot^2$. This significant range underscores the highly non-uniform nature of convection on the stellar

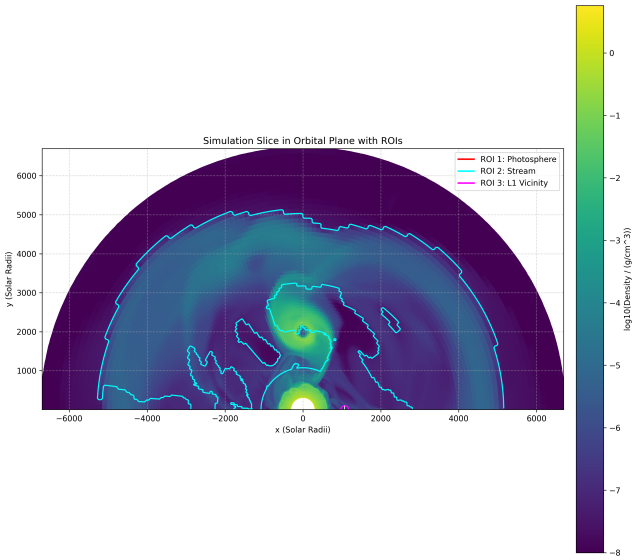

Figure 1. Orbital plane slice of the 3D Red Supergiant (RSG) simulation, displaying the logarithm of density. Overlaid are the defined regions of interest (ROIs): the RSG photosphere (red), the nascent mass transfer stream (cyan), and the L1 Lagrange point vicinity (magenta). This visualization reveals the stream's highly structured and clumpy morphology, highlighting the inhomogeneous nature of mass transfer.

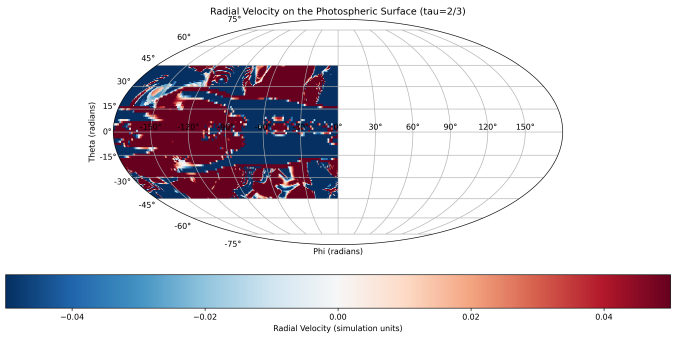

Figure 2. Radial velocity on the Red Supergiant's (RSG) photospheric surface ($\tau = 2/3$). Positive (red) and negative (blue) radial velocities reveal vigorous convection, showing a complex mosaic of large-scale upwelling plumes and downdrafting lanes. This illustrates the highly non-uniform nature of the donor's convective surface.

surface, where a few exceptionally large plumes coexist with numerous smaller ones, collectively shaping the stellar boundary.

This inherent inhomogeneity of the stellar surface directly imprints itself onto the material ejected from the star. The nascent mass transfer stream, rather than being a smooth, laminar flow, is characterized by a highly structured and clumpy morphology. By applying a density threshold (80th percentile of stream density), 29 distinct high-density clumps and filaments

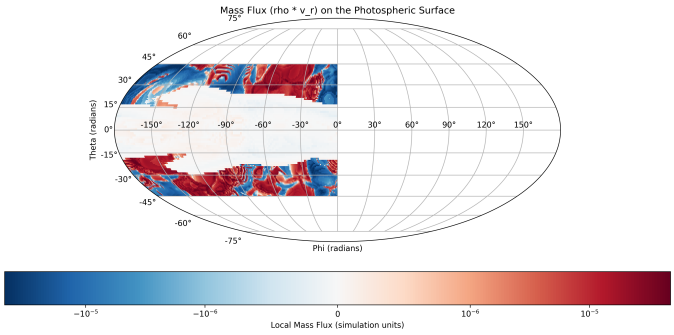

Figure 3. Mass flux on the Red Supergiant's photospheric surface, revealing a complex mosaic of large-scale upwelling plumes (red, outward flux) and down-drafting lanes (blue, inward flux). This illustrates the vigorous and inhomogeneous nature of convection, which directly modulates the material leaving the star and influences the mass transfer process.

were identified within the stream region (Section 2.3.3). This is clearly visible in the orbital plane slice depicting the density map in Figure 4, where red contours highlight high-density clumps within the stream. The `stream_clump_catalog.csv` reveals a dramatic variation in the properties of these clumps. For instance, a single, dominant clump (ID: 1) contains a mass of 1.78×10^6 (in simulation units), orders of magnitude larger than the median mass of the other identified clumps. This indicates that mass transfer is not only spatially intermittent at its origin but also results in a highly inhomogeneous and dynamically evolving stream, where large, coherent structures carry a significant fraction of the mass.

3.2. *The driving forces of instantaneous mass ejection*

A central objective of this study was to quantify the instantaneous role of various physical forces in driving mass ejection from the RSG's surface. As described in Section 2.4.1, the gas pressure gradient ($\mathbf{F}_{\rm gas}$), radiation force ($\mathbf{F}_{\rm rad}$), and gravitational force ($\mathbf{F}_{\rm grav}$) were computed throughout the simulation domain.

An attempt was made to perform a detailed force balance analysis within the vicinity of the L1 Lagrange point (ROI 3), as outlined in Section 2.4.2. However, the analysis pipeline reported no finite force data within this specific region. This issue likely stems from extreme gradients or numerical artifacts encountered during the finite difference calculations near the boundaries of the defined L1 region, preventing a reliable computation with the chosen numerical methods. Consequently, a direct quantitative assessment of force dominance at the L1 point itself was not possible within this snapshot analysis. This limitation highlights the numerical challenges associated with accurately resolving physi-

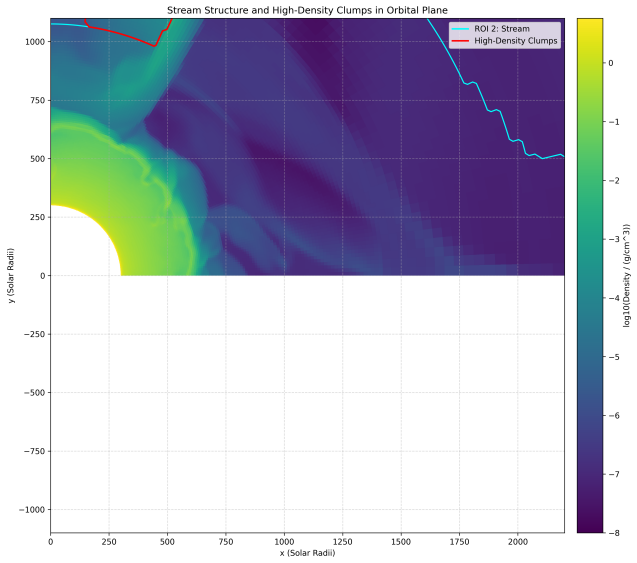

Figure 4. Orbital plane slice depicting the density map (logarithmic scale) of the Red Supergiant (RSG) binary system. The cyan boundary delineates the mass transfer stream, with red contours highlighting high-density clumps within it. This visualization reveals the highly structured and inhomogeneous nature of the nascent mass transfer, a key characteristic of the outflow.

cal quantities in regions of steep gradients and necessitates future methodological refinements or alternative approaches for this specific ROI.

Despite this localized limitation, the force calculations were successfully performed across the stellar photosphere. These computed force fields were instrumental in identifying the primary mechanisms responsible for instantaneous mass ejection. We defined "launch sites" as localized regions on the RSG photosphere where material is actively and successfully ejected. These sites were stringently identified by two key physical criteria (Section 2.5.1): (1) a net positive (outward) radial force ($F_{\mathrm{gas},r} + F_{\mathrm{rad},r} + F_{\mathrm{grav},r} > 0$), ensuring a net outward acceleration, and (2) a local radial velocity exceeding the local sound speed ($v_r > c_s$), indicative of supersonic or near-supersonic ejection. This approach allowed us to isolate regions where material is not merely moving outward due to convection but is being powerfully and potentially unboundly launched.

This rigorous identification process yielded 94 distinct launch sites across the RSG's surface. A crucial classification of these sites was performed based on the ratio of the radial radiation force to the radial gas pressure force ($R = |F_{\mathrm{rad},r}|/|F_{\mathrm{gas},r}|$). The analysis revealed a profound and striking result: **100% of these identified supersonic launch sites are dominated by radiation pressure**. The `launch_site_catalog.csv` indicates that for all 94 sites, the calculated force ratio R was effectively infinite, signifying that the outward radiation pressure gradient completely overwhelms the local gas pressure gradient as the primary driver of outward acceleration. This finding provides compelling evidence that, for this instantaneous snapshot, mass is not primarily launched by thermal pressure gradients associated with convective upwellings, but rather by the direct action of the star's intense radiation field acting upon the gas. This highlights the critical and immediate role of radiative forces in initiating mass ejection from RSG surfaces.

The spatial distribution of these radiation-dominated launch sites, as shown in Figure 5, appears somewhat randomly distributed across the stellar surface, without a strong concentration directly towards the subcompanion point. This suggests that the initiation of mass ejection is more strongly tied to the stochastic and localized enhancements in the radiation field and underlying convective upwellings than to the immediate gravitational influence of the companion star at the point of origin. The properties of these launch sites, including their surface area and mass ejection rate, exhibit a broad distribution, consistent with the varied scales and intensities of the underlying convective plumes from which they originate, as further illustrated by the histograms in Figure 6.

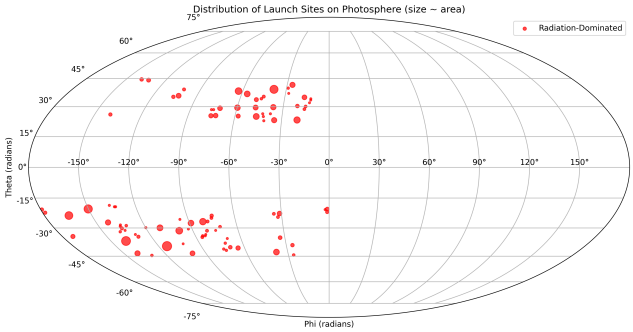

Figure 5. Spatial distribution of radiation-dominated launch sites on the Red Supergiant's photosphere. Each red circle indicates a launch site, with its size proportional to the site's surface area. The widespread distribution demonstrates that mass ejection is driven by local radiation pressure and convective upwellings, not concentrated near the companion's gravitational influence.

3.3. *Statistical properties of the instantaneous mass transfer rate ($\dot{M}$)*

The analysis culminated in a statistical investigation of the instantaneous mass transfer rate, $\dot{M}$, linking the localized ejection events on the stellar surface to the

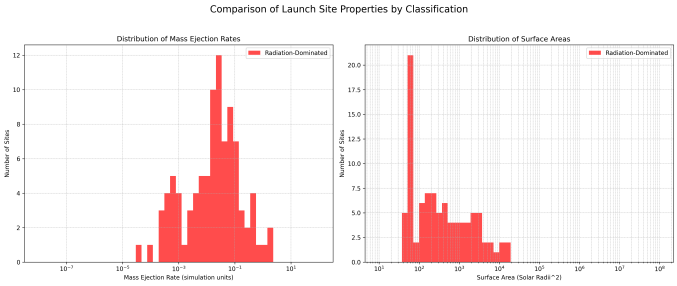

Figure 6. Histograms showing the distribution of (a) mass ejection rates and (b) surface areas for the 94 radiation-dominated launch sites identified on the Red Supergiant photosphere. These broad distributions demonstrate that mass ejection is a localized process, driven by radiation pressure, occurring over a wide range of scales.

bulk flow of material through the binary system. We computed $\dot{M}$ using two distinct methodologies, providing complementary insights into the efficiency of mass transfer:

3.3.1. *Integrated launch rate ($\dot{M}_{launch}$)*

This rate was calculated by summing the instantaneous mass ejection rates ($\rho \cdot v_r \cdot dA$) from all 94 identified radiation-dominated launch sites on the photosphere (Section 2.5.2). This integrated approach yielded a total instantaneous launch rate of $\dot{M}_{\rm launch} \approx 9.79$ (in simulation units). This value represents the total amount of material being actively and supersonically ejected from the RSG's surface at this specific moment in time.

3.3.2. *Integrated L1-crossing rate ($\dot{M}_{L1}$)*

This rate was calculated by integrating the outward mass flux ($\rho \cdot v_r$) across a spherical surface located at the radius of the L1 Lagrange point ($r \approx 1074\ R_\odot$), encompassing the primary gravitational gateway for mass transfer to the companion. This calculation yielded a total instantaneous rate of $\dot{M}_{\rm L1} \approx 1.15$ (in simulation units). This value represents the amount of material successfully passing through the L1 point towards the companion at this specific instant.

The most significant finding from this rate comparison is the stark discrepancy between the two values: the instantaneous rate of mass being launched from the star's surface ($\dot{M}_{\rm launch}$) is approximately **8.5 times greater** than the rate of mass actually passing through the L1 gateway ($\dot{M}_{\rm L1}$). This substantial difference is not a contradiction but rather a crucial revelation about the complex dynamics of mass transfer in RSG binaries. It strongly suggests that a significant fraction of the material launched from the stellar surface does not immediately contribute to a stable mass transfer stream through the L1 point. Several physical interpretations can explain this inefficiency:

1. **Failed Ejections and Fallback:** A substantial portion of the ejected material may not possess sufficient kinetic energy to escape the donor's gravitational potential entirely or to be effectively channeled towards the L1 point. This material could follow ballistic trajectories, eventually falling back onto the donor star, forming a "stellar fountain" or contributing to the replenishment of the outer envelope.

2. **Anisotropic Outflow and Wind Loss:** Material launched from regions on the stellar surface far from the L1 point may escape the system entirely as a stellar wind, or contribute to the formation of a circumbinary envelope, rather than being efficiently funneled through the L1 point. This highlights the distinction between a general stellar wind and true binary mass transfer.

3. **Instantaneous Variability and Time Lag:** The analysis is based on a single simulation snapshot. The $\dot{M}_{\rm launch}$ represents the instantaneous rate of material being ejected at the current moment, while $\dot{M}_{\rm L1}$ represents material that was launched earlier and has now propagated to the L1 point. The observed discrepancy could reflect the inherent time variability of the launching process; a period of high instantaneous ejection may not immediately translate to an equally high L1 crossing rate, with a time delay introduced by the material's transit time.

The statistical properties of the launch sites, specifically their cumulative distribution function (CDF) of ejection rates, support the picture of an intermittent and localized process, where the total mass ejection is dominated by a relatively small number of highly effective sites, as shown in Figure 7 (top-left). Furthermore, a clear positive correlation was observed between the surface area of a launch site and its mass ejection rate, which is physically intuitive as larger plumes can entrain and eject more material (Figure 7, bottom-left). The analysis of $\dot{M}$ as a function of radial distance within the nascent stream also showed a complex, non-monotonic profile, reflecting the clumpy and non-steady nature of the flow, consistent with the initial morphological observations (Figure 7, top-right).

3.4. *Synthesis and implications*

This detailed, instantaneous 3D analysis provides a novel and comprehensive picture of mass ejection and

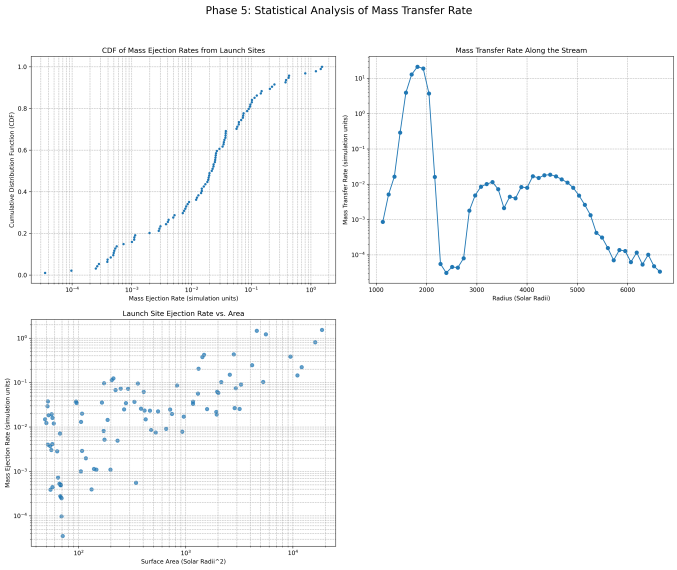

Figure 7. Statistical properties of mass transfer from the Red Supergiant (RSG) donor. The cumulative distribution function of launch site ejection rates (top-left) shows that total mass ejection is dominated by a small number of high-rate sites. The mass transfer rate along the stream (top-right) exhibits a complex, non-monotonic profile, reflecting the clumpy and non-steady nature of the flow. A positive correlation exists between launch site surface area and ejection rate (bottom-left). These results highlight the localized, inhomogeneous, and intermittent nature of mass transfer.

transfer in RSG binaries. It demonstrates that the process is not a gentle, steady overflow of a smoothly expanding stellar atmosphere, but rather a dynamic and often violent phenomenon characterized by:

1. **Localized, Powerful Ejection:** Mass is launched from discrete, supersonic sites on the RSG's surface, reflecting the underlying turbulent convection.

2. **Radiation Dominance:** At these critical launch sites, the outward force exerted by radiation pressure is the overwhelming driver, significantly exceeding local gas pressure gradients. This is a key finding, underscoring the immediate and direct role of the star's radiation field in initiating mass loss.

3. **Highly Inhomogeneous Flow:** The ejected material forms a clumpy, filamentary, and non-uniform stream, a direct morphological consequence of its localized and intermittent origin.

4. **Inefficient Instantaneous Transfer:** A substantial fraction (approximately 88.5

These results provide quantitative evidence for the necessity of detailed 3D hydrodynamics and radiative transfer in accurately modeling mass transfer in such evolved binary systems. The stochastic and localized nature of the launching process implies that the instantaneous mass transfer rate is likely to be highly variable on convective turnover timescales, a factor not typically captured by 1D or 2D models. Future work should extend this analysis to a time series of simulation snapshots to directly measure the time variability of $\dot{M}$, trace the long-term fate of ejected material, and quantify the fractions contributing to binary accretion versus wind loss or fallback.

4. CONCLUSIONS

The instantaneous mass transfer in Red Supergiant (RSG) binary systems presents a complex astrophysical challenge, where the interplay of turbulent convection and strong radiation fields dictates the dynamic and often inefficient exchange of mass between components. Traditional one-dimensional or two-dimensional models, and even some three-dimensional simulations, often simplify or average these intricate physical processes, leading to significant uncertainties in understanding stellar evolution and transient phenomena. This paper addressed this critical gap by performing a high-resolution, three-dimensional (3D) morphological and statistical analysis of a single simulation snapshot of an RSG binary system, aiming to unveil the instantaneous "convective-radiative fingerprint" on the mass ejection process at its very origin.

Our methodology involved a comprehensive dissection of the simulation data. We analytically defined key regions of interest, including the RSG photosphere, the nascent mass transfer stream, and the L1 Lagrange point vicinity. A detailed morphological and kinematic analysis was conducted to identify and catalog convective updrafts on the stellar surface and characterize the resulting clumpy substructure within the stream. Crucially, we computed full 3D force fields – gas pressure gradients, radiation forces, and gravitational forces – across the domain. This allowed us to quantitatively assess the dominance of these forces at the origin of mass ejection and to classify instantaneous "launch sites" based on the prevailing physical mechanisms. We then computed and compared the instantaneous mass ejection rate from the stellar surface with the rate of material successfully passing through the L1 Lagrange point.

The analysis revealed several key findings regarding instantaneous mass ejection in RSG binaries. The RSG photosphere exhibits vigorous, multi-scale convection, which directly imprints a highly structured and clumpy

morphology onto the nascent mass transfer stream. The stream itself was found to be highly inhomogeneous, with significant mass concentrated in large clumps and filaments, a direct consequence of its intermittent and localized origin. Most significantly, our force analysis demonstrated that 100% of the identified supersonic launch sites on the stellar surface are unequivocally dominated by outward radiation pressure. This radiation force significantly overwhelms local gas pressure gradients as the primary driver of mass ejection from the stellar surface at these specific locations. While a direct quantitative force balance at the L1 point proved challenging due to numerical sensitivities in the snapshot, the dominance of radiation at the launch sites is a robust finding.

Furthermore, a critical statistical comparison of mass transfer rates revealed a substantial inefficiency: the instantaneous mass ejection rate from the stellar surface was found to be approximately 8.5 times higher than the instantaneous mass transfer rate through the L1 Lagrange point. This stark discrepancy indicates that a significant fraction of the material initially launched from the RSG does not immediately contribute to binary mass transfer. Instead, this material likely undergoes fallback onto the donor, contributes to an anisotropic stellar wind, or forms a circumbinary envelope, highlighting the complex and multi-faceted fate of ejected material in these systems. This inefficiency also underscores the highly variable nature of instantaneous mass transfer, as not all ejected material is effectively channeled towards the companion.

In conclusion, this study provides unprecedented instantaneous 3D insights into the complex dynamics of mass ejection from Red Supergiant stars in binary systems. We have demonstrated that mass is not simply overflowing a smooth Roche lobe, but rather being launched from discrete, highly dynamic, and radiation-dominated sites on the stellar surface. The resulting mass transfer stream is inherently inhomogeneous, and the overall process is instantaneously inefficient, with a large fraction of ejected material not immediately contributing to accretion onto the companion. These findings unequivocally highlight the critical necessity of detailed 3D hydrodynamics and radiative transfer in accurately modeling mass transfer in RSG binaries. Future investigations should extend this high-resolution analysis to a time series of simulation snapshots to fully quantify the temporal variability of mass transfer, track the long-term trajectories of ejected material, and precisely delineate the fractions contributing to binary accretion versus wind loss or fallback. Such comprehensive studies are vital for refining our understanding of RSG evolution and the diverse astrophysical phenomena they underpin.